Nucleic Acids Research, 2005, Vol. 33, No. 11 ***3447–3454***
doi:10.1093/nar/gki626

Monitoring tat peptide binding to TAR RNA by solid-state ^{31}P–^{19}F REDOR NMR

Greg L. Olsen, Thomas E. Edwards[1], Pritilekha Deka, Gabriele Varani, Snorri Th. Sigurdsson[2] and Gary P. Drobny*

Department of Chemistry, University of Washington, Seattle, WA 98195-1700, USA, [1]Division of Basic Sciences, Fred Hutchinson Cancer Research Center, 1100 Fairview Avenue North, Seattle, WA 98109, USA and [2]Science Institute, University of Iceland, Dunhaga 3, IS-107 Reykjavik, Iceland

Received February 24, 2005; Revised and Accepted May 13, 2005

ABSTRACT

Complexes of the HIV transactivation response element (TAR) RNA with the viral regulatory protein tat are of special interest due in particular to the plasticity of the RNA at this binding site and to the potential for therapeutic targeting of the interaction. We performed REDOR solid-state NMR experiments on lyophilized samples of a 29 nt HIV-1 TAR construct to measure conformational changes in the tat-binding site concomitant with binding of a short peptide comprising the residues of the tat basic binding domain. Peptide binding was observed to produce a nearly 4 Å decrease in the separation between phosphorothioate and 2′F labels incorporated at A27 in the upper helix and U23 in the bulge, respectively, consistent with distance changes observed in previous solution NMR studies, and with models showing significant rearrangement in position of bulge residue U23 in the bound-form RNA. In addition to providing long-range constraints on free TAR and the TAR–tat complex, these results suggest that in RNAs known to undergo large deformations upon ligand binding, ^{31}P–^{19}F REDOR measurements can also serve as an assay for complex formation in solid-state samples. To our knowledge, these experiments provide the first example of a solid-state NMR distance measurement in an RNA–peptide complex.

INTRODUCTION

Characterization of RNA structure and dynamics is critical to understanding interactions of RNA with regulatory proteins and with potential RNA-targeted ligand molecules. Elucidation of the mechanisms and specificity of complex formation entails determination of the range of motions and conformations sampled by the RNA en route to the bound state (1). However, in certain RNA systems, experimental limitations or sample difficulties have thus far precluded acquisition of key information about the complexes. The interaction of the HIV-1 transactivation response element (TAR) RNA with the viral regulatory protein tat is an example of this: although binding of tat to this RNA motif has been shown to be essential for viral replication, and a wide array of biophysical and biochemical techniques have consequently been applied to the description of the structure (2–7) and motions (8–13) of both free- and tat-bound TAR, much remains to be learned about the interaction [for reviews see (14,15)]. Owing to difficulties in preparing properly folded tat protein or suitable samples of protein–TAR complex, solution NMR and X-ray investigations to date have studied simplified models of this system. While these studies have produced high-resolution RNA structures for complexes of HIV-2 TAR with argininimide (5), and of HIV-1 TAR with tat peptides (2,3,6), argininimide (2,3) and a variety of small molecules (16–19), peptide motion has thus far precluded the determination of high-resolution structures for bound peptides or a peptide–HIV-1 TAR complex, and the contacts tat makes with the TAR-binding site have not been directly observed.

Well-established solid-state NMR (SSNMR) techniques are readily available to address many of the aspects of this interaction that are not tractable by other means. SSNMR methods can provide long-range constraints in TAR and determine the conformation of bound peptides and can study motions on a wide range of timescales. Use of such experiments, however, necessitates parallel experiments to confirm proper formation of the appropriate RNA–ligand complex. One approach to the verification of complex formation in solid-state samples is to monitor a conformational change by measuring the distance

*To whom correspondence should be addressed. Tel: +1 206 685 2052; Fax: +1 206 685 8665; Email: drobny@chem.washington.edu

© The Author 2005. Published by Oxford University Press. All rights reserved.

The online version of this article has been published under an open access model. Users are entitled to use, reproduce, disseminate, or display the open access version of this article for non-commercial purposes provided that: the original authorship is properly and fully attributed; the Journal and Oxford University Press are attributed as the original place of publication with the correct citation details given; if an article is subsequently reproduced or disseminated not in its entirety but only in part or as a derivative work this must be clearly indicated. For commercial re-use, please contact journals.permissions@oupjournals.org

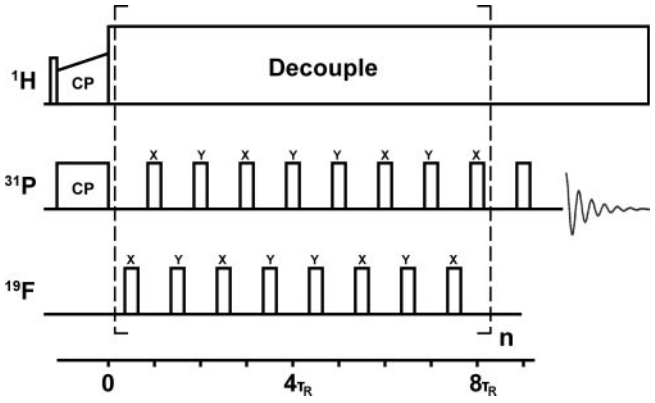

Figure 1. REDOR pulse sequence used to measure ^{19}F–^{31}P dipolar couplings. Initial phosphorus magnetization is produced by cross polarization from ^{1}H to ^{31}P. Application of a series of alternating rotor-synchronized fluorine and phosphorus 180° pulses dephases ^{31}P transverse magnetization, resulting in a reduced ^{31}P signal. The extent of dephasing observed is determined by the ^{19}F–^{31}P dipolar couplings. Comparison of this reduced signal with a reference signal obtained in the absence of the fluorine dephasing pulses allows the determination of the dipolar coupling, and thereby, direct extraction of the internuclear separation between ^{19}F and ^{31}P labeled sites.

between isotopic labels introduced at the binding site. When labels can be positioned such that binding is known or expected to result in a large change in the inter-label separation, observation of predicted changes in this distance following ligand addition gives evidence of complex formation in the sample.

Measurement of specific distance changes of sufficient magnitude to support claims of complex formation requires a method that can directly measure long distances (>5 Å) between isotopic labels in nucleic acids. The standard SSNMR technique for heteronuclear distance measurements is the rotational echo double resonance (REDOR) experiment [(20,21); for reviews see also (22,23)]. REDOR allows direct measurement of dipolar couplings between isotopic label pairs. Rf pulses applied during magic angle sample spinning (Figure 1) are used to restore the effects of selected dipolar interactions, dephasing the magnetization of any observed nuclei coupled to the irradiated spins in proportion to their respective internuclear separations. Decay in the ratio of this signal (S) to a reference signal (S_0) acquired in the absence of dephasing pulses is monitored as a function of the number of applied dephasing pulses ('dephasing time'), then fit to simulation to allow determination of the dipolar coupling constant and the corresponding internuclear distance.

REDOR has been used to make internuclear distance measurements in structural studies of numerous biological systems. Recent applications include studies of drug–DNA and enzyme–nucleotide complexes, illustrating the utility of the method for investigation of binding interactions of nucleic acids (24,25). ^{31}P–^{19}F REDOR has been used to determine distances of up to 13 Å in nucleic acids (26,27) and up to 16 Å in proteins (28). As distance constraints acquired using SSNMR experiments, such as REDOR, are frequently longer than those measurable using high-resolution NMR, SSNMR studies can also often provide a useful complement to X-ray or NOE/RDC-based methods of structure determination, aiding in refinement of global conformation in structures obtained by these or other methods.

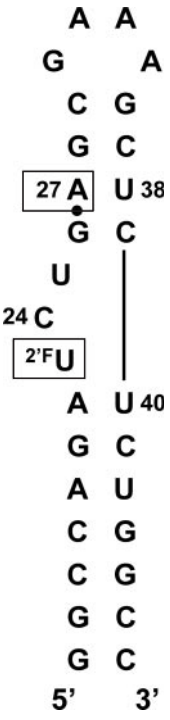

Figure 2. Apical region of TAR RNA, showing 29-residue construct used in the present work. The hexanucleotide upper loop of wild-type TAR has been replaced with the stable GAAA tetraloop. Label positions within the RNA are shown as follows: $^{2'F}$U indicates 2′-fluoro-2′-deoxyuridine (at bulge residue U23), and the dot between G26 and A27 denotes a phosphorothioate (pS) linkage.

In the present work, we use ^{31}P–^{19}F REDOR experiments to measure the change in the distance between ^{19}F and ^{31}P labels in the binding region of the HIV-1 TAR RNA (Figure 2) following binding of the tat-derived peptide $_{47}$YGRKKR-RQRRR$_{57}$. The distance between a 2′F label introduced at bulge residue U23 and a phosphorothioate 5′ of A27 was observed to change significantly, from 10.3 Å in the unbound RNA to 6.6 Å following binding of the peptide. Both distances are comparable with those obtained previously in solution NMR-based models of free TAR and the TAR–tat complex, and are consistent with the presence of intact complex in the solid-state sample.

MATERIALS AND METHODS

Sample preparation

TAR RNA. The TAR RNA 29mer 5′-GGCCAGA$^{2'F}$UCUG-(pS)AGCGAAAGCUCUCUGGCC-3′ (where pS indicates a phosphorothioate label) was purchased from Dharmacon (Lafayette, CO) and deprotected according to the manufacturer's instructions. The sample was checked for homogeneity using analytical denaturing PAGE and used without further purification. An aliquot of 1.07 μmol of the RNA was dissolved in 430 μl buffer (50 mM NaCl, 10 mM sodium cacodylate, pH 5.5), then frozen using liquid nitrogen, lyophilized and transferred to the MAS rotor (final composition 10% NaCl, and 4.7% cacodylate, respectively, by weight upon lyophilization).

Tat peptide. The 11mer tat peptide $_{47}$YGRKKRRQRRR$_{57}$ was synthesized on an Applied Biosystems 433A peptide synthesizer using standard fmoc chemistry, then cleaved and deprotected by stirring in a 95% TFA, 2.5% triisopropylsilane, 2.5% H_2O solution for 2.5 h. The resin was filtered off, and the TFA/product solution reduced to 2 ml under reduced pressure. The peptide was isolated by precipitation in cold (0°C) tert-butyl methyl ether and collected by centrifugation. The sample was then resuspended in cold tertbutyl methyl ether and recentrifuged. After three such reprecipitations, the sample was allowed to dry overnight at room temperature. The crude peptide was then purified by reverse-phase high-performance liquid chromatography using a Rainin Dynamax 25 × 250 mm preparatory C18 column [40 min linear gradient, from 2 to 50% solvent B (solvent A, 0.1% TFA in H_2O; solvent B, CH_3CN) flow rate 10 ml/min], quantitated using UV/vis (tyrosine ε_{275} = 1405 cm^{-1} mol^{-1}) and characterized using electrospray MS. TOCSY solution NMR spectra of a sample of wild-type TAR taken before and after addition the of the purified tat peptide produced diagnostic spectral shifts shown previously to be indicative of complex formation (3) (data not shown).

Complex formation. The RNA–peptide complex was formed as follows: the lyophilized TAR sample was re-dissolved in 500 µl sterile filtered H_2O. About 1.2 equivalents (1.284 µmol) of the purified peptide were dissolved in 500 µl sterile filtered H_2O. Both solutions were incubated at 37°C for 10 min, then combined by dropwise addition of the peptide solution to the RNA solution. The mixture was then returned to the heat block and held at 37°C for 10 min with frequent, gentle vortexing. An aliquot of 500 µl H_2O was added, and the solution was kept at 37°C for a further 50 min with continued gentle vortexing. A small amount of precipitate was observed to form following mixing and was retained in the sample. The solution was allowed to cool to room temperature, then frozen using liquid nitrogen, lyophilized and returned to the MAS rotor.

NMR spectroscopy

All experiments were performed on a homebuilt spectrometer at 4.7 Tesla field (200 MHz proton Larmor frequency), using a homebuilt triply-tuned HFP MAS probe. All measurements were made at room temperature (26°C), with magic angle spinning at 6493 Hz. Rf field strengths were regulated to within ±1%, spinning speed to within ±3 Hz and sample temperatures to within ±2°C. All REDOR experiments employed XY-8 phase cycling on both the ^{31}P and the ^{19}F channels (Figure 1) (29). Custom made 4 mm zirconia rotor barrels were purchased from O'Keeffe Ceramics. Samples were confined to the middle 10 mm of the 22 mm rotor. Rotor tips and end caps were prepared in-house.

Unbound RNA sample. Proton Rf fields were 48 kHz (initial π/2 pulses) and 94 kHz (CW decoupling). Cross-polarization employed a linear proton ramp, from 50 to 71 kHz field, with a 1.5 ms contact time. Phosphorus and fluorine rf pulse fields were 47 and 62 kHz, respectively. A total of 256 points were acquired, with a dwell time of 25 µs. Two REDOR data sets were acquired: three REDOR S and S_0 data point pairs were taken at 6.16 ms (5 REDOR cycle) intervals, and two additional REDOR point pairs were taken at 4.93 ms (4 REDOR cycle) intervals. Acquisition time in each case was 6.4 ms and recycle delay was 2 s. The first data set consisted of 122 880 scans for each REDOR S or S_0 data point, recorded in 6 144 or 12 288 scan blocks, for a total experiment time of 420 h. The second dataset consisted of 61 440 scans for each REDOR data point, recorded in a single experiment, for a total time of 140 h.

Bound RNA–peptide sample. Proton rf fields were 47 kHz (initial π/2 pulses), 51–73 kHz (ramped CP) and 106 kHz (CW proton decoupling). Phosphorus and fluorine rf pulse fields were 47 and 66 kHz. CP contact time, acquired points and dwell time used were the same as for the unbound sample. Four REDOR S and S_0 data point pairs were taken, at 1.23 ms (1 REDOR cycle) intervals. (Owing to rapid dephasing, this experiment was adjusted to collect S and S_0 points at the shorter intervals.) A total of 147 456 scans were acquired for each REDOR S or S_0 data point, in 19 individual 4096 to 14 336 scan data sets (19–65 h each; total experiment time 672 h), then summed. Acquisition time and recycle delay were again 6.4 ms and 2 s, respectively. TOCSY spectra of free and bound TAR RNA were collected at 500 MHz on a Bruker Avance spectrometer using DIPSI-2 mixing (60 µs) (30). Data were collected in ~12 h on a sample dissolved in 100% D_2O. Chemical shift identifications were accomplished based on published values (3,4) and on the characteristic changes that occur upon complex formation (3). Data were processed using UXNMR (Bruker) and analyzed with SPARKY (University of California, San Francisco).

Data processing

Data processing was performed using in-house NMR processing software (Gullringen: a computer program for the estimation of molecular properties from NMR experiments; T. Karlsson and G. P. Drobny, manuscript in preparation.) All simulations were performed using SIMPSON (31), with pulse widths, phases, field strengths and spinning speeds corresponding to the experimental NMR parameters described above. Ideal cross polarization and proton decoupling were assumed, and relaxation was ignored. Powder averaging for REDOR dephasing simulations used crystal file ZCW232 with 10 gamma angles and a maximum time step (maxdt) of 1.0 µs. Simulations were repeated using rep2000 and ZCW4180, with 100 gamma angles and maxdt 0.5 to check for convergence. As inclusion of simulated long-distance ^{31}P–^{31}P homonuclear dipolar interactions representing couplings of pS A27 to adjacent backbone phosphates in the RNA was found to produce negligible effects on dephasing, these were omitted from subsequent simulations of the REDOR data. Reduced chi-squared plots were used to determine best-fit distances and error bounds (90% confidence intervals).

RESULTS AND DISCUSSION

TAR RNA adopts distinct conformations in the presence and absence of tat

Given its well-established critical role in HIV replication and corresponding potential as an anti-viral drug target, the TAR–tat complex is one of the most extensively studied RNA–protein interactions. Efficient HIV-1 replication requires the interaction of the virally encoded tat protein with the TAR

element, a short stem–loop consisting of the first 59 nt at the 5′ end of the viral RNA transcript (32–35). The apical region of TAR (Figures 2 and 3) contains two short, A-form helical regions (2,4,35), whose junction at a 3 nt UCU bulge serves also as the tat binding site (32,36,37). Tat is a small basic protein, whose size in different viral isolates varies from 86 to 101 residues (38), the first 72 of which are required for transactivational activity (39). In the absence of tat, production of full-length RNA transcripts is severely attenuated. Binding of tat to the TAR motif during transcription is associated with dramatically increased production of full-length viral RNA transcripts (32–34). While structures of tat or tat peptides in complex with TAR have not yet been determined, X-ray and high-resolution NMR studies have been able to obtain local RNA conformations at the binding interface and have shown binding of tat peptides and argininimide to produce significant structural alterations in TAR.

In unbound TAR, the presence of the bulge nucleotides generates a distortion of the RNA at the junction of the upper and lower helices: solution NMR studies find the unpaired bases U23 and C24 to be stacked continuously above A22 (2,4). This disturbance to the helix is accommodated by a looping out of U25 and a widening of the major groove (4,40), and results in an approximately 50° average bend in the inter-helical angle (Figure 3A) (4,9,41–43). Solution NMR, CD and transient electric birefringence experiments indicate that tat binding straightens and stabilizes TAR (3,4,6,12,42,44). Binding of tat to the RNA has been shown to be mediated by a short arginine-rich region ($_{49}$RKKRRQRRR$_{57}$), which provides direct contacts with the TAR bulge binding site (33,34,36,37). Previous work has shown that RNA structural requirements for TAR binding by tat-derived peptides spanning this basic binding region, or by argininimide alone, mirror the requirements seen for binding and transactivation by the intact tat protein, suggesting that binding of peptides or argininimide induces a conformational change at the TAR bulge very similar to that generated by binding of the full protein (18,32–34,36,37,40,45–52).

Accommodation of the three unpaired bulge residues is accomplished by different means in the tat-bound RNA (Figure 3B and D). Binding is accompanied by unstacking of U23 and C24 and looping out of the three bulge nucleotides, allowing the upper and lower helices surrounding the bulge to stack coaxially, TAR to straighten and an arginine binding pocket to form (2–4,6,12,18,42,52). Modeling based on high-resolution NMR and chemical modification studies suggests that this TAR conformational change is initiated by the insertion of tat or argininimide guanidinium groups into the RNA major groove, resulting in a reorganization of key functional groups at the binding interface (2–4,18,40,52,53).

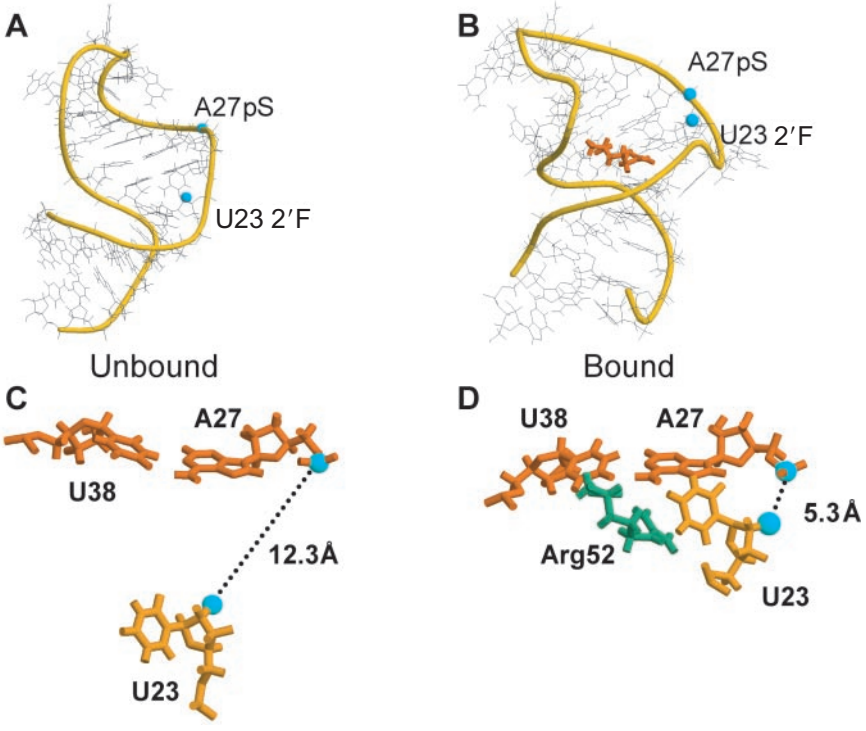

Figure 3. (A and B) Conformational changes in TAR upon tat peptide binding. The phosphate backbone is represented by yellow ribbons, highlighting rearrangements of the bulge residues generated by peptide binding. Blue spheres denote ^{19}F U23 and pS A27 label positions used in the present work. Illustrations and distances shown are adapted from solution NMR-derived models of the free and peptide-bound RNA (5,21). (**A**) Unbound conformation (PDB #1ANR, model one). (**B**) Bound conformation (PDB #1ARJ, model one.) Tat residue arg52, which provides key contacts with the RNA, is shown in orange. The RNA has straightened from the unbound conformation, residues C24 and U25 are looped out of the helix, and residue U23 has shifted to a new position adjacent to G26 and A27. (C and D) Rearrangements at TAR bulge binding site upon tat peptide binding. Blue spheres again denote ^{19}F U23 and pS A27 label sites. (**C**) Close-up of unbound conformation, showing relative positions of U23, A27 and U38, and the inter-label separation monitored in the present study (PDB #1ANR, model one; ^{19}F-pS inter-label separation is 12.3 Å in this model). (**D**) Close-up of bound conformation. Tat residue arg52 is shown in green. TAR accommodation of the tat peptide results in a significant repositioning of U23, drawing it into close proximity to A27 and U38, accompanied by a large decrease in separation between the ^{19}F U23 and pS A27 label positions (PDB #1ARJ, model one.) Following binding, the ^{19}F–pS distance has decreased to 5.3 Å in the model shown.

In particular, binding has been shown to be accompanied by a marked shift in position of bulge residue U23, situating it adjacent to G26 and A27, possibly as part of a U23:A27:U38 base triple (Figure 3D) (2–6,52,54). It has also been shown by EPR spectroscopy that the mobility of U23 and U38 is dramatically reduced upon peptide binding, consistent with the role of these nucleotides in complex formation (11,13). These rearrangements, most notably the large change in position undergone by bulge residue U23, suggest several suitable diagnostic labeling sites for SSNMR observation of complex formation.

^{31}P–^{19}F REDOR solid-state NMR measurements

To monitor conformational changes accompanying the formation of the RNA–peptide complex in the solid-state sample, we selected a label pair positioned astride the bulge region, whose separation within TAR was shown by earlier solution NMR studies to undergo a sizeable change upon complex formation (Figure 3C and D). We performed ^{31}P–^{19}F REDOR distance measurements on samples of a 29-residue TAR construct, in which 2′ fluorine and phosphorothioate labels were introduced at U23 and 5′ of A27, respectively, and in which the wild-type CUGGGA upper loop was replaced with a stabilizing GAAA tetraloop (Figure 2). This labeling choice offers several benefits. Recent high-resolution NMR studies of the structural effects of phosphorothioate substitutions in an RNA hairpin and in DNA/RNA duplexes found little or no change in conformation when pS labels were introduced in helical regions, as is the case for A27 in the TAR construct used in the present work (55–57). Furthermore, 2′F sugar moiety labeling provides a structural reporter more directly sensitive to backbone conformational changes than would be available through a base-labeling approach. A gel mobility-shift binding assay comparing (2′F U23, pS A27) TAR and the corresponding unlabeled wild-type TAR 29mer showed that both TAR constructs bind the tat 11mer with similar affinities (data not shown.)

Unbound TAR. Representative ^{31}P reference (S_0) spectra corresponding to the initial REDOR S/S_0 point for the unbound and bound TAR RNA are shown in Figure 4. The phosphorothioate and backbone phosphate peaks show approximate linewidths of 9 and 6 ppm, respectively. In the free RNA, best fits to the REDOR data showed the measured $^{2'F}$U23-pS A27 inter-label distance to be 10.3 ± 0.6 Å (Figure 5). This result is consistent with previously reported solution NMR results for two similar unbound HIV-1 TAR constructs (4). In that work, Aboul-ela and co-workers used solution NMR-derived constraints to generate energy-minimized model structures for the TAR apical region, using samples of the 29 nt RNA construct 5′-GGCAGAUCUGAGCCUGGGAGCUCUCUGCC-3′ and a related 27mer, in which the CUGGGA loop had been replaced by a UUCG tetraloop. In the 20 published models (PDB #1ANR), the mean inter-label separation corresponding to our label positions was 11.1 Å, while the separation itself ranged from 8.1 to 14.2 Å (SD 1.7 Å.) The distance observed in the lyophilized sample is thus in statistical agreement with the distance obtained for comparable TAR constructs in solution. While it is clearly not possible to exclude the possibility that multiple conformers are present in the sample without further experiments, the monotonic dephasing seen in the REDOR data is consistent with the presence of a unique distance, hence it is likely that the lyophilized sample contains predominantly a single conformer of the unbound RNA.

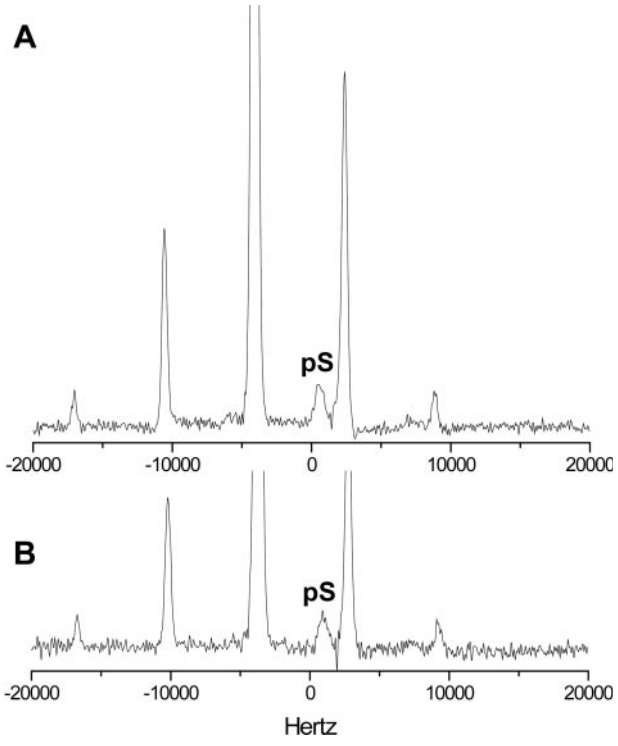

Figure 4. ^{31}P MAS spectra of the unbound (**A**) and bound (**B**) TAR RNA. Plots were generated without linebroadening and show reference (S_0) spectra corresponding to REDOR S/S_0 points acquired at 1.23 ms. In each spectrum, the phosphorothioate peak (pS A27) monitored to measure REDOR dephasing is denoted by 'pS'; the remaining peaks are isotropic and spinning sideband peaks owing to unmodified backbone phosphates.

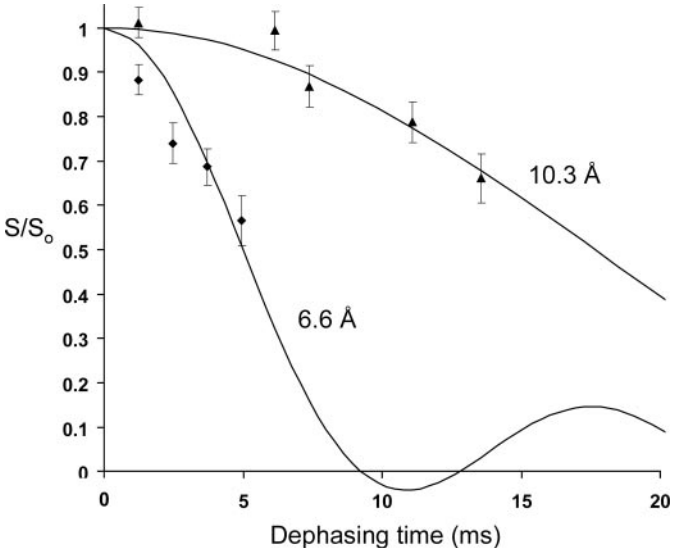

Figure 5. REDOR dephasing curves for unbound TAR RNA and TAR–tat peptide complex. Diamonds mark data for the unbound RNA, and triangles for the complex. Solid lines represent simulated dephasing corresponding to 10.3 and 6.6 Å, respectively. All simulations used SIMPSON, as described in the text.

TAR–tat complex. As noted above, binding of peptides similar to the undecamer tat peptide used in this study has been suggested to produce a conformational change in TAR similar to that generated by the full protein. REDOR measurements taken following the addition of the tat peptide $_{47}$YGRKKRRQRRR$_{57}$ indicated that the binding site in the TAR construct had undergone a substantial rearrangement. The distance between the ^{19}F and ^{31}P labels in the binding region was observed to drop by 3.7 Å, from 10.3 Å in the unbound RNA to 6.6 ± 0.7 Å following introduction of the peptide (Figure 5). Although signal limitations prevent quantitative treatment of phosphorothioate lineshape changes, little apparent change in linewidth or chemical shift was observed following peptide binding. In both the unbound and bound spectra, the phosphorothioate peak is slightly broader than the superimposed phosphate peak produced by the remaining 28 nt of the crystalline RNA sample. The absence of significant changes in phosphorothioate linewidth or chemical shift following peptide binding is consistent with previous solution NMR studies, showing the label site to be in a relatively well-defined helical region in both the unbound and bound RNAs. The dephasing data for the bound RNA suggest that more than one distance may be present, indicative of possible structural heterogeneity in the sample. While in the present experiments the perturbation to the dephasing is small, such a possibility cannot be excluded, as the effects of lyophilization on biological samples have not as yet been well characterized.

While earlier structural studies of TAR have shown U23 to be repositioned significantly as a result of complex formation, to a new position near G26 and A27, these reports have differed over what that position is. In structures determined by several groups, the pyrimidine ring of bulge residue U23 was found to participate in a base triple with residues A27 and U38 of the upper helix (2,6,52). In contrast, Aboul-ela *et al*. found instead that the base was situated nearer to A26 (3). In a set of 20 published energy-minimized model structures (PDB #1ARJ) for the TAR apical region in complex with a peptide containing both the tat basic binding domain and core region, or with argininimide, and using samples of the same 29 and 27 nt RNA constructs used in their subsequent study of the free RNA, Aboul-ela and co-workers found the mean inter-label separation corresponding to our label positions to be 4.8 Å, while the separation this time ranged from 3.7 to 6.1 Å (SD 0.74 Å). While the distance observed in the lyophilized sample thus shows a significant decrease with respect to the distance seen in the free RNA, as expected, it is slightly larger than that obtained for comparable bound TAR constructs in solution. Although disagreement remains over the precise placement of U23 in bound TAR, in both types of proposed bound TAR structure U23 adopts relatively well-defined positions near G26 or A27. Comparison of the solution NMR results of Aboul-ela *et al*. for the free and tat-bound RNA suggests that complex formation should result in a distance change of at least 2.0 Å, and possibly considerably larger. Coordinate files for alternate structures of the HIV-1 complex are not available. In either case, and as we have observed in the present study, a decrease in the distance between our label sites is expected, indicating that the 3.7 Å distance change observed in the REDOR measurements is consistent with the presence of intact complex in the solid-state sample.

CONCLUSION

In summary, REDOR SSNMR measurements on lyophilized samples of a 29-residue TAR RNA construct showed binding of a tat-derived peptide to result in a 3.7 Å decrease in the separation between ^{31}P and ^{19}F labels introduced at the binding site, from 10.3 Å in the free RNA to 6.6 Å in the bound RNA. The results of previous structural studies of the free HIV-1 TAR and of tat peptide–TAR complexes obtained using solution NMR are supported by our data, which indicate that a sizeable rearrangement occurred at the TAR RNA binding site following peptide addition, consistent with the presence of the peptide–TAR complex in the solid-state sample. To our knowledge, these experiments provide the first example of an SSNMR distance measurement in an RNA–peptide complex. SSNMR studies of the structure and dynamics of the TAR–tat system are under way and will be reported in due course.

ACKNOWLEDGEMENTS

The authors gratefully acknowledge James Gibson, Gil Goobes, Elizabeth Louie, Jennifer Popham and Vinodhkumar Raghunathan for many helpful and stimulating discussions, and the Drobny research group for critical review of the manuscript. This work was supported by a grant from the National Institutes of Health (NIH/NIBIB RO1 EB03152-O5). Funding to pay the Open Access publication charges for this article was provided by National Institutes of Health (NIH/NIBIB RO1 EB03152-O5).

Conflict of interest statement. None declared.

REFERENCES

1. Leulliot,N. and Varani,G. (2001) Current topics in RNA–protein recognition: control of specificity and biological function through induced fit and conformational capture. *Biochemistry*, **40**, 7947–7956.
2. Puglisi,J.D., Tan,R., Calnan,B.J., Frankel,A.D. and Williamson,J.R. (1992) Conformation of the TAR RNA–arginine complex by NMR spectroscopy. *Science*, **257**, 76–80.
3. Aboul-ela,F., Karn,J. and Varani,G. (1995) The structure of the human immunodeficiency virus type-1 TAR RNA reveals principles of RNA recognition by Tat protein. *J. Mol. Biol*., **253**, 313–332.
4. Aboul-ela,F., Karn,J. and Varani,G. (1996) Structure of HIV-1 TAR RNA in the absence of ligands reveals a novel conformation of the trinucleotide bulge. *Nucleic Acids Res*., **24**, 3974–3981.
5. Brodsky,A.S. and Williamson,J.R. (1997) Solution structure of the HIV-2 TAR-argininamide complex. *J. Mol. Biol*., **267**, 624–639.
6. Long,K.S. and Crothers,D.M. (1999) Characterization of the solution conformations of unbound and Tat peptide-bound forms of HIV-1 TAR RNA. *Biochemistry*, **38**, 10059–10069.
7. Al-Hashimi,H.M., Gorin,A., Majumdar,A., Gosser,Y. and Patel,D.J. (2002) Towards structural genomics of RNA: Rapid NMR resonance assignment and simultaneous RNA tertiary structure determination using residual dipolar couplings. *J. Mol. Biol*., **318**, 637–649.
8. King,G.C., Harper,J.W. and Xi,Z. (1995) Isotope labeling for 13C relaxation measurements on RNA. *Methods Enzymol*., **261**, 437–450.
9. Al-Hashimi,H.M., Gosser,Y., Gorin,A., Hu,W., Majumdar,A. and Patel,D.J. (2002) Concerted motions in HIV-1 TAR RNA may allow access to bound state conformations: RNA dynamics from NMR residual dipolar couplings. *J. Mol. Biol*., **315**, 95–102.
10. Dayie,K.T., Brodsky,A.S. and Williamson,J.R. (2002) Base flexibility in HIV-2 TAR RNA mapped by solution ^{15}N, ^{13}C NMR relaxation. *J. Mol. Biol*., **317**, 263–278.

11. Edwards,T.E., Okonogi,T.M. and Sigurdsson,S.T. (2002) Investigation of RNA–protein and RNA–metal ion interactions by electron paramagnetic resonance spectroscopy: The HIV TAR–Tat motif. *Chem. Biol*., **9**, 699–706.
12. Pitt,S.W., Majumdar,A., Serganov,A., Patel,D.J. and Al-Hashimi,H.M. (2004) Argininamide binding arrests global motions in HIV-1 TAR RNA: comparison with Mg^{2+}-induced conformational stabilization. *J. Mol. Biol*., **338**, 7–16.
13. Edwards,T.E., Robinson,B.H. and Sigurdsson,S.T. (2005) Identification of amino acids that promote specific and rigid TAR RNA–Tat protein complex formation. *Chem. Biol*., **12**, 329–337.
14. Karn,J. (1999) Tackling Tat. *J. Mol. Biol*., **293**, 235–254.
15. Rana,T.M. and Jeang,K.T. (1999) Biochemical and functional interactions between HIV-1 Tat protein and TAR RNA. *Arch. Biochem. Biophys*., **365**, 175–185.
16. Faber,C., Sticht,H., Schweimer,K. and Rosch,P. (2000) Structural rearrangements of HIV-1 Tat-responsive RNA upon binding of neomycin B. *J. Biol. Chem*., **275**, 20660–20666.
17. Du,Z., Lind,K.E. and James,T.L. (2002) Structure of TAR RNA complexed with a Tat–TAR interaction nanomolar inhibitor that was identified by computational screening. *Chem. Biol*., **9**, 707–712.
18. Davis,B., Afshar,M., Varani,G., Murchie,A.I., Karn,J., Lentzen,G., Drysdale,M., Bower,J., Potter,A.J., Starkey,I.D. *et al*. (2004) Rational design of inhibitors of HIV-1 TAR RNA through the stabilisation of electrostatic 'hot spots'. *J. Mol. Biol*., **336**, 343–356.
19. Murchie,A.I., Davis,B., Isel,C., Afshar,M., Drysdale,M.J., Bower,J., Potter,A.J., Starkey,I.D., Swarbrick,T.M., Mirza,S. *et al*. (2004) Structure-based drug design targeting an inactive RNA conformation: exploiting the flexibility of HIV-1 TAR RNA. *J. Mol. Biol*., **336**, 625–638.
20. Gullion,T. and Schaefer,J. (1989) Rotational-echo double-resonance NMR. *J. Magn. Reson*., **81**, 196–200.
21. Gullion,T. and Schaefer,J. (1989) Detection of weak heteronuclear dipolar couplings by rotational-echo double-resonance nuclear magnetic resonance. *Adv. Magn. Reson*., **13**, 57–83.
22. Gullion,T. (1997) Measurement of heteronuclear dipolar interactions by rotational-echo, double-resonance nuclear magnetic resonance. *Magn. reson. rev*., **17**, 83–131.
23. Dusold,S. and Sebald,A. (2000) Dipolar recoupling under magic angle spinning conditions. In Webb,G. (ed.), *Annual Reports on NMR Spectroscopy*. Academic Press Inc., San Diego, Vol. 41, pp. 185–264.
24. Mehta,A.K., Shayo,Y., Vankayalapati,H., Hurley,L.H. and Schaefer,J. (2004) Structure of a quinobenzoxazine–G-quadruplex complex by REDOR NMR. *Biochemistry*, **43**, 11953–11958.
25. Jiang,Y.L., McDowell,L.M., Poliks,B., Studelska,D.R., Cao,C., Potter,G.S., Schaefer,J., Song,F. and Stivers,J.T. (2004) Recognition of an unnatural difluorophenyl nucleotide by uracil DNA glycosylase. *Biochemistry*, **43**, 15429–15438.
26. Merritt,M.E., Sigurdsson,S.T. and Drobny,G.P. (1999) Long-range measurements to the phosphodiester backbone of solid nucleic acids using 31P–19F REDOR NMR. *J. Am. Chem. Soc*., **121**, 6070–6071.
27. Olsen,G.L., Louie,E.A., Drobny,G.P. and Sigurdsson,S.T. (2003) Determination of DNA minor groove width in distamycin–DNA complexes by solid-state NMR. *Nucleic Acids Res*., **31**, 5084–5089.
28. Studelska,D.R., Klug,C.A., Beusen,D.D., McDowell,L.M. and Schaefer,J. (1996) Long-range distance measurements of protein binding sites by rotational-echo double resonance NMR. *J. Am. Chem. Soc*., **118**, 5476–5477.
29. Gullion,T., Baker,D.B. and Conradi,M.S. (1990) New, compensated Carr-Purcell sequences. *J. Magn. Reson*., **89**, 479–484.
30. Shaka,A.J., Lee,C. and Pines,A. (1988) Iterative schemes for bilinear operations—applications to spin decoupling. *J. Magn. Reson*., **77**, 274–293.
31. Bak,M., Rasmussen,J.T. and Nielsen,N.C. (2000) SIMPSON: a general simulation program for solid-state NMR spectroscopy. *J. Magn. Reson*., **147**, 296–330.
32. Dingwall,C., Ernberg,I., Gait,M.J., Green,S.M., Heaphy,S., Karn,J., Lowe,A.D., Singh,M. and Skinner,M.A. (1990) HIV-1 tat protein stimulates transcription by binding to a U-rich bulge in the stem of the TAR RNA structure. *EMBO J*., **9**, 4145–4153.
33. Calnan,B.J., Biancalana,S., Hudson,D. and Frankel,A.D. (1991) Analysis of arginine-rich peptides from the HIV Tat protein reveals unusual features of RNA–protein recognition. *Genes Dev*., **5**, 201–210.
34. Roy,S., Delling,U., Chen,C.H., Rosen,C.A. and Sonenberg,N. (1990) A bulge structure in HIV-1 TAR RNA is required for Tat binding and Tat-mediated *trans*-activation. *Genes Dev*., **4**, 1365–1373.
35. Muesing,M.A., Smith,D.H. and Capon,D.J. (1987) Regulation of mRNA accumulation by a human immunodeficiency virus *trans*-activator protein. *Cell*, **48**, 691–701.
36. Weeks,K.M., Ampe,C., Schultz,S.C., Steitz,T.A. and Crothers,D.M. (1990) Fragments of the HIV-1 Tat protein specifically bind TAR RNA. *Science*, **249**, 1281–1285.
37. Cordingley,M.G., LaFemina,R.L., Callahan,P.L., Condra,J.H., Sardana,V.V., Graham,D.J., Nguyen,T.M., LeGrow,K., Gotlib,L., Schlabach,A.J. and Colonno,R.J. (1990) Sequence-specific interaction of Tat protein and Tat peptides with the transactivation-responsive sequence element of human immunodeficiency virus type 1 *in vitro*. *Proc. Natl Acad. Sci. USA*, **87**, 8985–8989.
38. Myers,G., Korber,B.T., Foley,B.T., Jeang,K.-T., Mellors,J.W. and Wain-Hobson,S. (eds) (1996) *Human Retroviruses and AIDS 1996: A Compilation and Analysis of Nucleic Acid and Amino Acid Sequences*. Theoretical Biology and Biophysics Group, Los Alamos National Laboratory, Los Alamos, NM, pp. III-11–III-26.
39. Frankel,A.D., Biancalana,S. and Hudson,D. (1989) Activity of synthetic peptides from the Tat protein of human immunodeficiency virus type 1. *Proc. Natl Acad. Sci. USA*, **86**, 7397–7401.
40. Weeks,K.M. and Crothers,D.M. (1991) RNA recognition by Tat-derived peptides: interaction in the major groove? *Cell*, **66**, 577–588.
41. Riordan,F.A., Bhattacharyya,A., McAteer,S. and Lilley,D.M. (1992) Kinking of RNA helices by bulged bases, and the structure of the human immunodeficiency virus transactivator response element. *J. Mol. Biol*., **226**, 305–310.
42. Zacharias,M. and Hagerman,P.J. (1995) The bend in RNA created by the *trans*-activation response element bulge of human immunodeficiency virus is straightened by arginine and by Tat-derived peptide. *Proc. Natl Acad. Sci. USA*, **92**, 6052–6056.
43. Long,K.S. (1997). Characterization of a human immunodeficiency virus TAR RNA element and its complex with a Tat-derived peptide. PhD Thesis, Yale University, New Haven, CT.
44. Tan,R. and Frankel,A.D. (1992) Circular dichroism studies suggest that TAR RNA changes conformation upon specific binding of arginine or guanidine. *Biochemistry*, **31**, 10288–10294.
45. Dingwall,C., Ernberg,I., Gait,M.J., Green,S.M., Heaphy,S., Karn,J., Lowe,A.D., Singh,M., Skinner,M.A. and Valerio,R. (1989) Human immunodeficiency virus 1 tat protein binds *trans*-activation-responsive region (TAR) RNA *in vitro*. *Proc. Natl Acad. Sci. USA*, **86**, 6925–6929.
46. Roy,S., Parkin,N.T., Rosen,C., Itovitch,J. and Sonenberg,N. (1990) Structural requirements for trans activation of human immunodeficiency virus type 1 long terminal repeat-directed gene expression by tat: importance of base pairing, loop sequence, and bulges in the tat-responsive sequence. *J. Virol*., **64**, 1402–1406.
47. Sumner-Smith,M., Roy,S., Barnett,R., Reid,L.S., Kuperman,R., Delling,U. and Sonenberg,N. (1991) Critical chemical features in *trans*-acting-responsive RNA are required for interaction with human immunodeficiency virus type 1 Tat protein. *J. Virol*., **65**, 5196–5202.
48. Tao,J. and Frankel,A.D. (1992) Specific binding of arginine to TAR RNA. *Proc. Natl Acad. Sci. USA*, **89**, 2723–2726.
49. Loret,E.P., Georgel,P., Johnson,W.C.,Jr and Ho,P.S. (1992) Circular dichroism and molecular modeling yield a structure for the complex of human immunodeficiency virus type 1 *trans*-activation response RNA and the binding region of Tat, the *trans*-acting transcriptional activator. *Proc. Natl Acad. Sci. USA*, **89**, 9734–9738.
50. Weeks,K.M. and Crothers,D.M. (1992) RNA binding assays for Tat-derived peptides: implications for specificity. *Biochemistry*, **31**, 10281–10287.
51. Churcher,M.J., Lamont,C., Hamy,F., Dingwall,C., Green,S.M., Lowe,A.D., Butler,J.G., Gait,M.J. and Karn,J. (1993) High affinity binding of TAR RNA by the human immunodeficiency virus type-1 tat protein requires base pairs in the RNA stem and amino acid residues flanking the basic region. *J. Mol. Biol*., **230**, 90–110.
52. Puglisi,J.D., Chen,L., Frankel,A.D. and Williamson,J.R. (1993) Role of RNA structure in arginine recognition of TAR RNA. *Proc. Natl Acad. Sci. USA*, **90**, 3680–3684.
53. Calnan,B.J., Tidor,B., Biancalana,S., Hudson,D. and Frankel,A.D. (1991) Arginine-mediated RNA recognition: the arginine fork. *Science*, **252**, 1167–1171.

54. Tao,J., Chen,L. and Frankel,A.D. (1997) Dissection of the proposed base triple in human immunodeficiency virus TAR RNA indicates the importance of the Hoogsteen interaction. *Biochemistry*, **36**, 3491–3495.
55. Gonzalez,C., Stec,W., Reynolds,M.A. and James,T.L. (1995) Structure and dynamics of a DNA.RNA hybrid duplex with a chiral phosphorothioate moiety: NMR and molecular dynamics with conventional and time-averaged restraints. *Biochemistry*, **34**, 4969–4982.
56. Bachelin,M., Hessler,G., Kurz,G., Hacia,J.G., Dervan,P.B. and Kessler,H. (1998) Structure of a stereoregular phosphorothioate DNA/RNA duplex. *Nature Struct. Biol.*, **5**, 271–276.
57. Smith,J.S. and Nikonowicz,E.P. (2000) Phosphorothioate substitution can substantially alter RNA conformation. *Biochemistry*, **39**, 5642–5652.